1-1-2015

Nonthermal atmospheric pressure plasma enhances mouse limb bud survival, growth, and elongation.

Natalie Chernets
Electrical and Computer Engineering Department, Drexel University

Jun Zhang
Department of Orthopedic Surgery, Thomas Jefferson University; Department of Orthopedics, Second Hospital of Jilin University

Marla J Steinbeck
School of Biomedical Engineering, Science and Health Systems, Drexel University; Department of Orthopedic Surgery, Drexel University College of Medicine

Deepa S Kurpad
Department of Orthopedic Surgery, Thomas Jefferson University

Eiki Koyama
Division of Orthopedic Surgery, Children's Hospital of Philadelphia

See next page for additional authors

TISSUE ENGINEERING: Part A
Volume 21, Numbers 1 and 2, 2015

DOI: 10.1089/ten.tea.2014.0039

Nonthermal Atmospheric Pressure Plasma Enhances Mouse Limb Bud Survival, Growth, and Elongation

Natalie Chernets, PhD,[1] Jun Zhang, MD,[2,3] Marla J. Steinbeck, PhD,[4,5] Deepa S. Kurpad, MS,[2] Eiki Koyama, PhD,[6] Gary Friedman, PhD,[1] and Theresa A. Freeman, PhD[2]

The enhanced differentiation of mesenchymal cells into chondrocytes or osteoblasts is of paramount importance in tissue engineering and regenerative therapies. A newly emerging body of evidence demonstrates that appendage regeneration is dependent on reactive oxygen species (ROS) production and signaling. Thus, we hypothesized that mesenchymal cell stimulation by nonthermal (NT)-plasma, which produces and induces ROS, would (1) promote skeletal cell differentiation and (2) limb autopod development. Stimulation with a single treatment of NT-plasma enhanced survival, growth, and elongation of mouse limb autopods in an *in vitro* organ culture system. Noticeable changes included enhanced development of digit length and definition of digit separation. These changes were coordinated with enhanced Wnt signaling in the distal apical epidermal ridge (AER) and presumptive joint regions. Autopod development continued to advance for approximately 144 h in culture, seemingly overcoming the negative culture environment usually observed in this *in vitro* system. Real-time quantitative polymerase chain reaction analysis confirmed the up-regulation of chondrogenic transcripts. Mechanistically, NT-plasma increased the number of ROS positive cells in the dorsal epithelium, mesenchyme, and the distal tip of each phalange behind the AER, determined using dihydrorhodamine. The importance of ROS production/signaling during development was further demonstrated by the stunting of digital outgrowth when anti-oxidants were applied. Results of this study show NT-plasma initiated and amplified ROS intracellular signaling to enhance development of the autopod. Parallels between development and regeneration suggest that the potential use of NT-plasma could extend to both tissue engineering and clinical applications to enhance fracture healing, trauma repair, and bone fusion.

Introduction

Tissue engineering and regenerative medicine employs a variety of strategies to promote cell proliferation, differentiation, and tissue development of both *in vivo* and *in vitro* synthetic constructs. The application of external stimuli for the purpose of modifying cellular function is a key approach in tissue engineering. Recently, we reported that nonthermal (NT) dielectric barrier discharge (DBD) plasma treatment stimulated reactive oxygen species (ROS)–associated cell signaling to enhance both osteoblast and chondrocyte differentiation.[1] Results from this study led us to investigate the effects of NT-plasma treatment on the more complex *in vitro* tissue model of mouse limb autopod development. Enhancement of ROS signaling during development is supported by studies showing tail regeneration in *Xenopus*, and zebrafish is dependent on ROS production.[2,3] Parallels are known to exist between the blastema in regeneration and functionality of the apical epidermal ridge (AER) in autopod development. Thus, we hypothesized that engineering NT-plasma to produce the appropriate extracellular ROS would activate intracellular ROS-sensitive signaling pathways in the AER and enhance digit growth. In the course of these studies, insights into which pathways are necessary would be determined and could be applied to further enhance tissue regeneration.

Vertebrate limbs grow through the coordinated activity of numerous growth factor signaling pathways, including the Wnt, fibroblast growth factor (FGF), bone morphogenetic protein (BMP), Notch, and transforming growth factor-β pathways.[2–6] ROS play a primary role in mediating the activity of these factors and/or are integrally involved in regulating downstream

[1]Electrical and Computer Engineering Department, Drexel University, Philadelphia, Pennsylvania.
[2]Department of Orthopedic Surgery, Thomas Jefferson University, Philadelphia, Pennsylvania.
[3]Department of Orthopedics, The Second Hospital of Jilin University, Chang Chun, Jilin, China.
[4]School of Biomedical Engineering, Science & Health Systems, Drexel University, Philadelphia, Pennsylvania.
[5]Department of Orthopedic Surgery, Drexel University College of Medicine, Philadelphia, Pennsylvania.
[6]Division of Orthopedic Surgery, The Children's Hospital of Philadelphia, Philadelphia, Pennsylvania.

signaling pathways.[7] For example, a sustained increase in ROS levels is required for Wnt β-catenin signaling and the activation of one of its main downstream targets, fgf20.[8,9] In addition, naturally occurring oxidative spikes are observed in most of the transition stages throughout developmental and regenerative processes.[10,11] Furthermore, there is precedence for ROS production to both direct and enhance mesenchymal cell differentiation into either chondrocyte or osteoblast lineages.[12–14]

The roles of ROS in stem cell differentiation and regeneration described earlier are also directly applicable to development. For example, ROS involvement has been examined in transformation of the autopod during digit individualization. FGF, BMP, and ROS regulate interdigital cell death/apoptosis within the autopod, thereby restricting interdigit growth and promoting regression of interdigital tissue.[15] The ROS-induced oxidative stress associated with apoptosis of these cells is due to mitochondrial production of ROS, the production by nicotinamide adenine dinucleotide phosphate (NADPH) oxidase in response to growth factors, and a decrease in the expression of the antioxidant enzymes superoxide dismutase 1–3, catalase, and glutathione peroxidase 1–7.[16] Studies have shown that the addition of antioxidants prevents interdigit cell death.[17,18] In contrast within the digit, high levels of antioxidants are expressed to control oxidative stress, thereby promoting cell proliferation, growth, and differentiation.

In this study, we are employing an atmospheric pressure plasma known as DBD plasma.[19] This type of NT-plasma is produced when a high-voltage, time-varying waveform is applied between two electrodes in air separated by an insulator.[20] The insulator prevents current build-up, thus creating electrically safe plasma without a substantial temperature rise. Since the NT-plasma discharge occurs in air, it is a highly complex mix of reactive chemical species (i.e., nitric oxide [NO], ROS, oxygen singles, and ozone), free ions, visible, ultraviolet, and near-infrared light, electric fields, and electromagnetic (EM) radiation.[21] Therefore, determination of which single or combination of plasma components is responsible for the observed outcome is difficult to assess. In the development of limb autopods, one study showed that a 2 h treatment with EM field stimulated limb growth through increased proliferation and chondrocyte differentiation.[22] In clinical orthopedics, both pulsed EM fields and ultrasound have been shown to enhance bone formation in defects, fractures, and bone lengthening.[23,24]

The goal of this study was to advance our previous work in a cell culture system to the tissue level, using the limb autopod model, to determine whether NT-plasma could stimulate ROS-sensitive signaling pathways to enhance limb development. Here, we show that exposure to NT-plasma promotes mouse limb autopod survival, growth, and elongation. In addition, the changes induced by NT-plasma stimulation are mediated through ROS-associated signaling. Finally, this work provides a fundamental understanding of NT-plasma effects on developing tissues and its potential use as a treatment modality to enhance the development of biological substitutes both *in vitro* and *in vivo*.

Materials and Methods

Animals

Timed pregnant mice were ordered from Jackson laboratory to ensure that the embryos would be at gestational age E12 to E14. The mice either had a CD-1 genetic background or were β-catenin/TCF/LEF reporter transgenic mice [BAT-GAL transgenic mice—Tg(BAT-lacZ)] mice containing a lacZ gene under the control of seven consensus LEF/TCF-binding motifs upstream of a minimal promoter of the *Xenopus* siamois gene.[25] BAT-lacZ experiments were performed on a litter of nine pups with three pups collected at each time point at day 1, 2, and 5, after which staining for β-galactosidase was performed according to the standardized protocol by Lobe *et al.*[26] All animals were euthanized according to National Institutes of Health (NIH) guidelines for the care and use of laboratory animals, and all animal protocols were approved by the Institutional Animal Care and Use Committee (IACUC) at Thomas Jefferson University.

Explant cultures

Limb autopods from embryos of gestational ages E12.5 and E14.5 were isolated and cultured in Dulbecco's modified Eagle's medium (DMEM; Cellgro, ThermoFisher Scientific) using the method previously described.[3] The limbs were placed on a nylon membrane in 12-well plates and moistened with 220 μL of DMEM with no serum.[27] Approximately 1 h after isolation, NT-plasma or sham (limb positioned under electrode with no discharge) treatment was applied, to the left (NT-plasma) and right limb (sham) autopod from the same animal. Immediately after treatment, the limb was transferred to fresh DMEM. Eighteen hours later, the culture medium was changed to DMEM with 2% fetal bovine serum (FBS) (Invitrogen, Life Science Technologies) and supplemented with 100 U/mL penicillin,100 μg/mL streptomycin (Cellgro, ThermoFisher Scientific). This medium was changed daily thereafter for the 4–6 days of culture.

At the conclusion of the experiment, the limbs were fixed with 4% paraformaldehyde in phosphate-buffered saline and imaged to evaluate the length of the digits, the interdigital clefting, and the appearance of the cartilage. To more clearly visualize the cartilagenous elements, the limbs were stained with alcian blue.[28] Imaging was performed using an Olympus MVX10 microscope with an Olympus DP70 color camera (Olympus Corp.).

NT-plasma treatment

Limb autopods were treated with DBD plasma similar to the procedure described by Fridman *et al.*,[29] where the schematics, voltage, and current curves of the power supply (Plasma Power, LLC) are detailed. The treatment voltage, frequency, pulse width, and time were based on our previous publication.[1] Briefly, NT-plasma was generated using a microsecond pulsed voltage of 20 kV (peak to peak) with a pulse width of 10 μs, a typical rise rate of 5 V/ns, and a pulse repetition rate of 1000 Hz applied through a high-voltage electrode for 10 s. The high-voltage electrode was composed of an inner copper core surrounded by an outer insulating shell of acrylic, also detailed by Fridman *et al.*[29] (Fig. 1A). Before NT-plasma and sham treatments, each limb on the nylon membrane was transferred out of the DMEM from the 12-well plate to a new 35 mm plastic dish and rewetted with 220 μL of phenol red-free DMEM. The 35 mm dish was placed on a grounded metal plate, and the high voltage electrode was positioned 2 mm above the limb. The blue plasma discharge (5 mm) surrounded the autopod (2–3 mm)

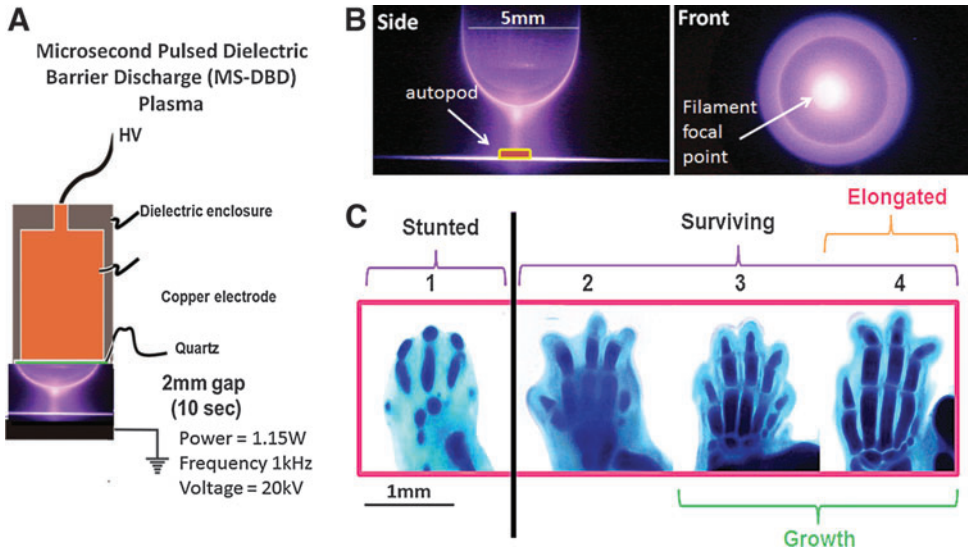

FIG. 1. Microsecond pulsed dielectric barrier discharge plasma treatment conditions. **(A)** Schematics of the nonthermal (NT)-plasma electrode applied to limb buds. **(B)** Picture of the NT-plasma electrode. *Left:* bottom view; *Right:* side view. **(C)** Assessment of digit development and growth of an alcian blue-stained E12.5 autopod using a defined Grading Scale: 1, stunted; 2–4, surviving; 3–4, growth; 4, elongation. Color images available online at www.liebertpub.com/tea

as shown in Figure 1B. Of note, plasma produced by this electrode is not uniform and filaments are formed intermittently during the plasma treatment, visible in Figure 1B as a brighter intensity in the central region of plasma. Filaments represent a more concentrated stream of plasma. Immediately after treatment, the limb on the nylon membrane was transferred to a new 12-well plate containing fresh DMEM. Sham treatment group was treated the same, but the high voltage was not applied.

Antioxidant treatments

The following inhibitors dissolved in dimethyl sulfoxide were used as anti-oxidant treatments: 2-(4-Carboxyphenyl)-4,4,5,5-tetramethylimidazoline-1-oxyl-3-oxide (CPTIO), 300 μM (Enzo Life Sciences); n-acetyl cysteine (NAC), 200 μM (Sigma-Aldrich); and 4-hydroxy-2,2,6,6-tetramethylpiperidin-1-oxyl (Tempol), 6 mM (Sigma-Aldrich). After isolation, the autopods were placed in DMEM with each inhibitor for 1 h before NT-plasma treatment. Just before NT-plasma treatment, limb medium was changed to 220 μL phenol red-free DMEM with no FBS supplemented with each inhibitor. Immediately after NT-plasma treatment, the limb was transferred to 220 μL of fresh DMEM with phenol red and no FBS, supplemented with inhibitors. Eighteen hours later, the culture medium was removed and 220 μL of DMEM and 2% FBS supplemented with inhibitors was added. This media with inhibitors was refreshed with each daily media change. The sham treatment group was treated the same but received no plasma treatment.

Assessment of limb autopod development

Limb autopod survival, growth, and development were assessed using a 1–4 grading system (Fig. 1C). A score of 1 indicates stunted growth (lack of survival) with no defined cartilage segments. A score of 2 indicates the autopod has survived, developed the first two distinct cartilagenous joint segments. A score of 3 indicates the autopod has undergone growth, developed three joint segments, and the metatarsal or metacarpal is approximately equal in length to the proximal phalange. A score of 4 indicates the autopod has undergone growth and elongation, has three or more joint segments, and the metatarsal or metacarpal is longer than the proximal phalange. The scores between contralateral pairs were calculated to determine the effectiveness of NT-plasma versus sham treatment. A pie chart was created to display the results between each pair of contralateral limbs by tallying which treatment received the higher score. Then, the scoring results[1–4] from all contralateral experiments were tabulated to provide an overall assessment of growth and development independent of the contralateral limb. A histogram was generated by tallying the scores for all limbs for each treatment NT-plasma or sham. Validation that contralateral limbs in organ culture perform equivalently was determined by evaluating 10 contralateral autopods cultured for 6 days without treatment. These results indicated no significant difference in the normal growth of contralateral limbs ($p = 1.00$).

Histology

Tissue samples were fixed overnight in 4% paraformaldehyde, dehydrated in a graded series of alcohols, and infiltrated and embedded in paraffin. Sections were cut at 6 μm and mounted on slides (Superfrost/Plus; Thermo Fisher Scientific). Cell and tissue morphology between treatments was compared using histological staining of limb sections with hematoxylin, eosin, and alcian blue (proteoglycan stain for cartilage).

Real-time polymerase chain reaction for differentiation markers and comparative analyses

Limb autopods were harvested at 24 or 144 h after sham or NT-plasma treatment. For each analysis, two autopods of each treatment group were pooled to create a sample in which RNA was isolated, and data from an n of 3 of these pooled samples were used to perform polymerase chain reaction (PCR) analysis. All harvested limbs were washed with diethylpyrocarbonate water before total RNA was isolated using the QiagenRNeasy® Micro kit (Qiagen). RNA yield was determined spectrophotometrically, and integrity was confirmed by gel electrophoresis. RNA was reverse transcribed and then amplified using the Superscript™ One-Step RT-PCR with Platinum Taq® (Invitrogen) kit. PCR products were analyzed by 1.0% agarose gel electrophoresis.

Template cDNA and gene specific primers were added to Fast SYBR Green master mix (Applied Biosystems), and mRNA expression was quantified using the MyIQ Real-Time PCR System (BioRad). The expression level of the housekeeping gene, β-actin was used to normalize the data presented. Melting curves were analyzed to verify the specificity of the reverse transcription (RT)-PCR and the absence of primer dimer formation. Each sample was analyzed in duplicate and included a template-free control. All the primers (Supplementary Table S1; Supplementary Data are available online at www.liebertpub.com/ten) used were synthesized by Integrated DNA Technologies, Inc.

Statistical analysis

Statistical analysis between groups was performed using a one-way ANOVA for normality and Student's *t*-test for continuous variables. A level of significance (α), or a *p*-value of less than 0.05, with a 95% confidence interval was determined. Representative data are presented as the mean ± standard error of the mean of individual samples from 2 to 10 independent analyses. For nonparametric data, Mann–Whitney U tests were used to evaluate differences.

Results

NT-plasma enhances limb autopod growth and development

To ascertain whether NT-plasma promotes growth and development of embryonic tissue, E12.5 mouse autopods were treated with a single NT-plasma treatment and then maintained in culture for approximately 6 days. Figure 2A shows representative, consecutive images of NT-plasma-enhanced digit development in an E12.5 autopod compared with its contralateral sham control (left treated with NT-plasma vs. right sham-treated control forelimbs or hind limbs). In developing embryos, hind limb maturation is delayed as compared with forelimb, by ~1 day. For example, cartilaginous development evaluated using alcian blue staining to show digit definition, length, and joint space illustrates that the initial digit segmentation occurs at 24 h in the forelimb as compared with 48 h of the hind limb (Fig. 2B). At these time points, NT-plasma-treated autopods showed increased lengthening of the distal segments, signifying accelerated digit growth of the fore and hind limbs when compared with sham controls. At 48 h (forelimb) and 72 h (hind limb), all digit segments were noticeably more defined, longer, and wider in response to NT-plasma treatment. At 72 h (forelimb) and 96 h (hind limb), NT-plasma-treated autopods displayed an additional distal segment with the appearance of the final joint space. In addition, at 144 h, both the NT-plasma-treated fore and hind limbs were noticeably larger, while the sham-treated autopods had stopped growing. Quantification of contralateral autopod growth shown in the pie chart in Figure 2C indicates that NT-plasma treatment promoted and enhanced growth in 76% of the autopods, as compared with only 5% increase after sham treatment; ($n = 21$; $p = 0.0003$). The remaining 19% of the limbs showed no difference between sham and NT-plasma treatments. To determine whether growth enhancement could be achieved with hydrogen peroxide (H_2O_2), a 30 s treatment with 200 μM and 1 mM H_2O_2 in DMEM was performed in place of NT-plasma treatment and no effect on limb growth was observed ($n = 9$, results not shown).

In addition, evaluation of autopod development was performed using a numerical scoring system of 1–4 and the growth status of each limb from every experiment was assessed independent of the contralateral limb. Briefly, in this scoring system, each individual limb received one of the following scores based on morphology and alcian blue staining: stunted, nonsurvival (1), survival (>1), growth (3,4), and elongation (4) (Fig. 1C). Results of E12.5 autopods ($n = 61$) limbs from all experimental groups treated with NT-plasma indicated that NT-plasma significantly improved the outcome of limb survival ($p = 0.01$), and increased limb elongation ($p = 0.001$), as compared with sham control (Fig. 2D; $n = 73$).

When the same experiments were repeated with E14.5 embryo limbs, a less dramatic but still significant increase in limb development was observed after NT-plasma treatment. Contralateral limb growth was enhanced for 60% of the NT-plasma treated autopods as compared with 23% after sham treatment (Fig. 2E; $n = 30$; $p = 0.03$). Seventeen percent of the time, there was no difference between the two treatments. Grading analysis of E14.5 autopods showed that NT-plasma treatment ($n = 39$) resulted in significantly increased elongation as compared with sham control ($n = 135$) (Fig. 2F; $p = 0.001$).

Increased chondrogenesis after NT-plasma treatment

To ascertain whether the enhanced growth observed was due to normal or aberrant chondrogenesis, we stained sections of the limb autopods treated with both NT-plasma and sham with H&E and alcian blue. Morphological formation of the joint region and alcian blue staining of proteoglycan appeared normal in sham and NT-plasma-treated digits (Fig. 3A; $n = 9$). Chondrocytes in the proximal segment of the sham-treated digit were entering the prehypertrophic stage, based on the larger size, greater cellular spacing, and decrease in proteoglycan (white arrowhead). This typically precedes the formation of the primary center of ossification in the diaphysis. In contrast, chondrocytes from the NT-plasma-treated digit were immature and contained large amounts of proteoglycan. Even more striking was the much larger cartilage phalangeal segments in the NT-plasma-treated digit. A white line with double arrows marks the joint between the first and second phalanges in both sections. In the sham-treated digit, the adjacent joint spaces (white arrow) can be clearly observed; whereas in the NT-plasma-treated digits, there is no evidence of the next joint space, due to the increased segment length.

Quantitative RT-PCR was used to assess chondrogenesis and other molecular events associated with the accelerated development in response to NT-plasma (Fig. 3). In E12.5 autopods, at 24 h post-NT-plasma treatment, alkaline phosphate (ALKP), catalase (CAT), endothelial nitric oxide synthase (eNOS), and BMP2 expression were increased twofold above control ($p < 0.05$). BMP4 and runt-related transcription factor 2 (Runx2) were increased 12-fold and 8-fold, respectively ($p < 0.05$), whereas FGF-2 showed no increase. Even more significant increases were observed at 144 h for ALKP (6-fold), CAT (14-fold), and BMP2 (3.5-fold) ($p < 0.05$). eNOS remained increased twofold above

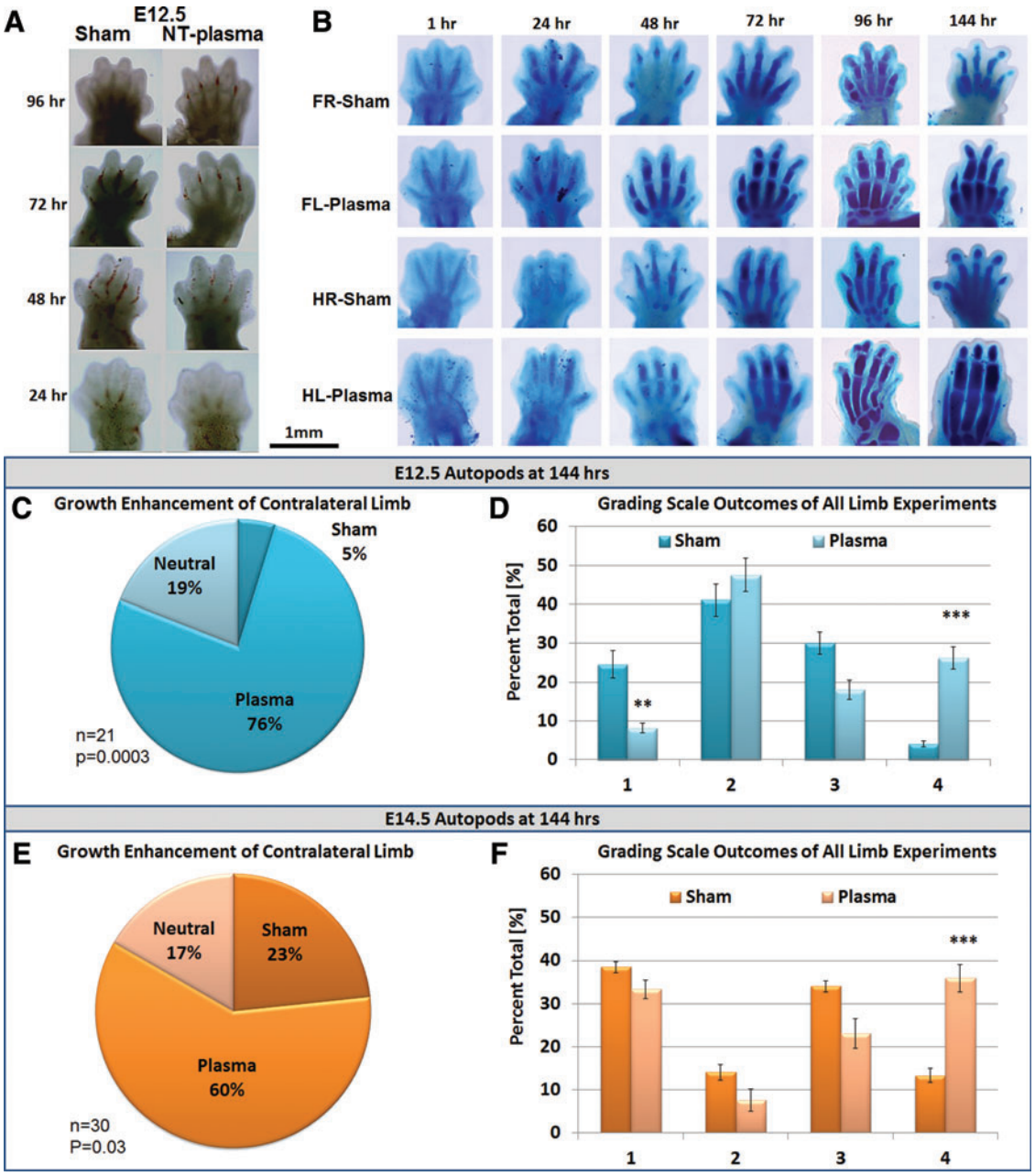

FIG. 2. NT-plasma treatment enhances thriving, growth, and elongation in mouse limb autopod development. **(A)** Consecutive images of NT-plasma enhanced digit development in an E12.5 autopod compared with its contralateral sham control. **(B)** Alcian blue (cartilaginous elements) stained fore and hindlimb autopods after NT-plasma or sham treatment. **(C)** Contralateral limb growth enhancement comparisons for sham and NT-plasma-treated E12.5 autopods. **(D)** Grading scale results for all limb experiments showing NT-plasma enhanced survival, growth, and elongation compared with sham-treated E12.5 autopods. **(E)** Contralateral limb growth enhancement comparisons for sham and NT-plasma-treated E14.5 autopods. **(F)** Grading scale results for all limb experiments showing NT-plasma enhanced elongation compared with sham treatment of E14.5 autopod. $^{**}p < 0.01$, $^{***}p < 0.001$. Color images available online at www.liebertpub.com/tea

control at 144 h, and both BMP4 and Runx2 evidenced consistent elevated expression at 24 and 144 h. Up-regulation of chondrogenic transcripts confirmed the morphologic changes associated with chondrocyte differentiation in the autopod. The increased expression of CAT emphasized the importance of antioxidant expression within the digit for cell proliferation, growth, and differentiation.[15]

NT-plasma treatment increases H_2O_2 production by cells within the limb autopod

To directly assess the production of ROS by limb cells, E12.5 autopods were stained with dihydrorhodamine (DHR), a dye that becomes fluorescent after a reaction with H_2O_2. Figure 4 shows representative images after 24 or

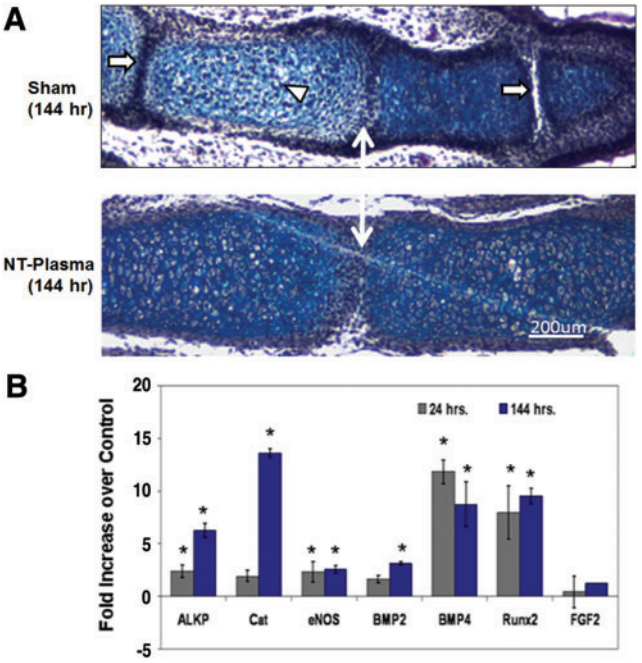

FIG. 3. Histology and quantitative real time-polymerase chain reaction were used to assess chondrogenesis and molecular events associated with the accelerated development. **(A)** A representative, hematoxylin and eosin (H&E) and alcian blue stained sections of middle phalanges from sham and NT-plasma-treated limb autopods. A *white double arrow line* marks the first joint space. The *white arrows* mark adjacent joint spaces, and the *white arrowhead* marks prehypertrophic chondrocytes in the sham control. **(B)** At 24 h post-NT-plasma treatment, alkaline phosphate (ALKP), catalase (CAT), endothelial nitric oxide synthase (eNOS), and bone morphogenetic protein 2 (BMP2) expression increased twofold above control. BMP4 and runt-related transcription factor 2 (Runx2) increased 12-fold and 8-fold, respectively, and fibroblast growth factor (FGF)-2 showed no increase. One hundred forty-four hours later, increases for ALKP (6-fold), CAT (14-fold), and BMP2 (3.5-fold). eNOS remained increased twofold above control at 144 h. BMP4 and Runx2 showed a relatively consistent elevated expression at 24 and 144 h. The results are expressed as the mean ± standard deviation ($n = 3$ [two limbs pooled per sample], $^*p < 0.05$). Color images available online at www.liebertpub.com/tea

144 h post-NT-plasma treatment. Of note, since the cells within the epithelium are translucent, positive cells observed in these images are present not only at the surface but also several hundreds of microns into the tissue. The unstained autopod (without DHR) at 24 h shows low-level autofluorescence of collagen; while in both the sham and NT-plasma-treated autopods, H_2O_2-positive cells are localized to the interdigital region as well as throughout the epithelial surface. H_2O_2-positive cells in these regions are consistent with localized cellular apoptosis as the limb grows and the digits separate. The transmitted light image shows the limb autopod features at this time point. In addition, the NT-plasma-treated autopod contains a layer of H_2O_2-positive cells lining the cartilaginous digits that are not observed in the sham control (Fig. 4; white arrows). A high magnification image of the NT-plasma-treated area shows epithelial damage due to filaments generated by plasma (white arrowheads), and the presence of H_2O_2-positive cells in this region. NT-plasma-treated autopods stained with both DHR and propidium iodide (PI—dead cells) indicate that cell death is primarily localized to the immediate area of filament damage, where H_2O_2- and PI-positive cells co-localized (Supplementary Fig. S1). However, outside of this region, very few H_2O_2-positive cells showed signs of cell death.

By 144 h, a characteristic overgrowth of epithelium is observed in the sham control, visualized by the cloudy green autofluorescence of collagen in the epithelium. In contrast, the NT-plasma-treated autopod shows bright punctate fluorescence of individual H_2O_2-positive cells. A patterning of these cells is observed within the interdigit regions and throughout the less developed epithelium (white arrows). The high magnification image of the NT-plasma-treated area shows initial healing of the treated area (white arrowheads) and the presence of H_2O_2-positive cells.

Representative images comparing the presence of H_2O_2-positive cells at the digit tip in sham and NT-plasma-treated limbs at 24 and 144 h are shown in Figure 5A. In response to NT-plasma treatment, an increased number of H_2O_2-producing cells were observed in the tip region of each digit at 24 h (Fig. 5A). These cells were localized behind a specialized region known as the AER, where mesenchymal cells receive signals from the AER, directing their differentiation into chondrocytes.

Increased Wnt-signaling in the AER and presumptive joints after NT-plasma

To determine whether signaling activity is also increased at the AER in response to NT-plasma and H_2O_2 production, E12.5 contralateral limb autopods from the Bat LacZ Wnt-signaling reporter mouse were treated with NT-plasma or sham-treated. To visualize the expression and distribution of wnt, the limbs were stained with lacZ (blue). Twenty-four hours after NT-plasma treatment, enhanced lacZ staining is evident in the posterior thumb region (white circle), where wnt is known to function as a regulator of anterior-posterior patterning (Fig. 5B).[30] Forty-eight hours after treatment, digit separation is more evident, and the AER of each digit stains more intensely for lacZ in response to NT-plasma compared with sham control (black arrows). At 120 h, AER wnt staining remains elevated in the NT-plasma-treated autopod and digit separation and elongation is more evident in these limbs. Joints are also beginning to form at this stage and can be identified by early Wnt signaling (white arrows) in the presumptive joint spaces. The NT-plasma-treated autopod clearly shows an increased number of joints compared with sham controls, indicating accelerated maturation of the cartilage anlage.

Antioxidant stunting of limb autopod development is partially rescued by NT-plasma

Inhibitors were used to evaluate the role of ROS and reactive nitrogen species (RNS) in mediating NT-plasma accelerated E12.5 mouse autopod development (Fig. 5C). NAC (200 μM) was used to maintain intracellular redox balance,[31] Tempol (6 mM), a membrane-permeable scavenger of both ROS and RNS, was used to prevent changes to intracellular oxidant levels,[32,33] and CPTIO (300 μM) was used as a chemical scavenger of NO (NO•).[34] Autopod

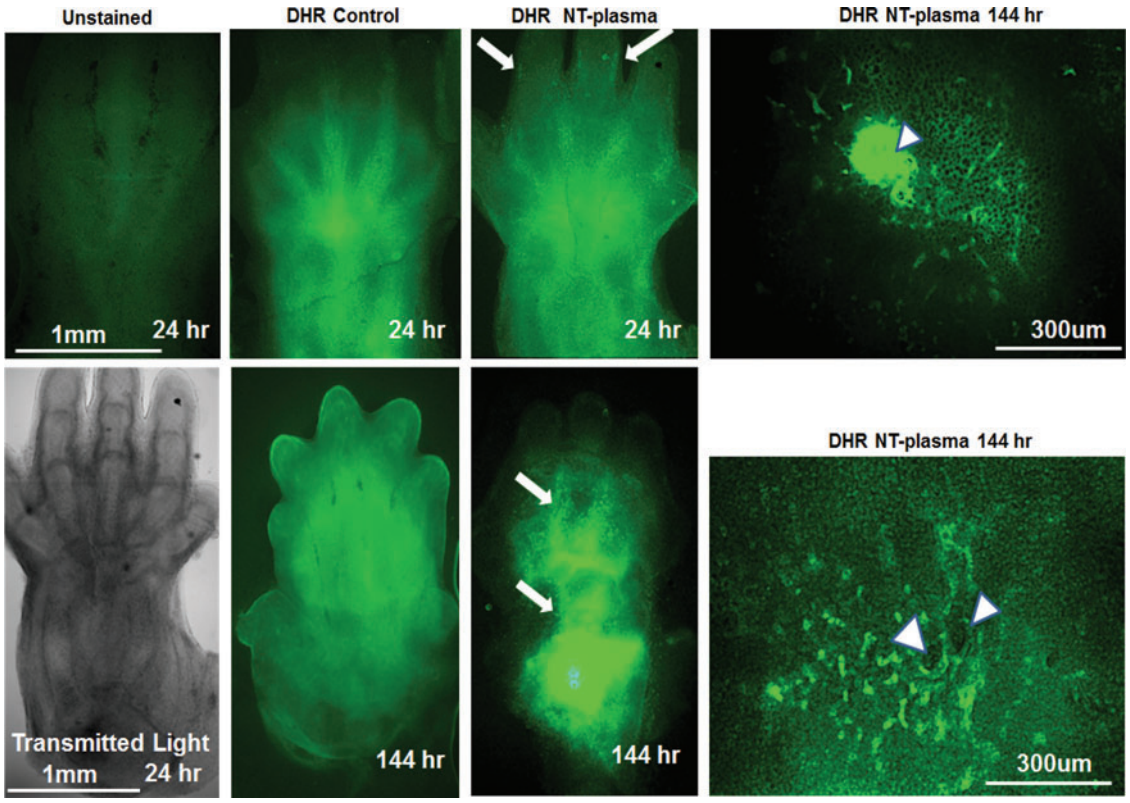

FIG. 4. NT-plasma treatment increases intracellular hydrogen peroxide (H_2O_2) in cells of the epithelium. DHR fluorescence 1 h after NT-plasma treatment; limb unstained and transmitted light images are shown to verify specificity of DHR and anatomical localization. Twenty-four hours later, control limb shows prominent H_2O_2 production in the interdigital spaces and NT-plasma-treated limbs show more defined H_2O_2 production next to the cartilage as the digits separate (*white arrows*). Additional staining is observed at the edges of the wrist and scattered throughout the epithelium. One hundred forty-four hours later, control autofluorescence of collagen within the forming epithelial skin overgrowth, and NT-plasma-treated limb with H_2O_2-positive cells throughout the epithelia and interdigital spaces (*white arrows*). Higher magnification images at 24 and 144 h show that the cells immediately surrounding the site of plasma filament damage (*white arrowheads*) continue to generate H_2O_2 after a single 10 s NT-plasma treatment. Color images available online at www.liebertpub.com/tea

morphogenesis was stunted by the pretreatment of the limbs with each antioxidant, confirming the importance of ROS and RNS in development. Inhibition of both ROS and RNS by Tempol completely stunted autopod development. However, removal of RNS by CPTIO had the least effect and mediation of ROS by NAC showed an intermediate effect. Interestingly, NT-plasma treatment partially rescued development, moderately enhancing digit morphogenesis even in the presence of these anti-oxidants.

Discussion

This work follows up on our previous report that NT-plasma treatment increased intracellular ROS production and promoted the expression of differentiation specific genes, synergistically enhancing both osteogenic and chondrogenic differentiation.[1] In this more complex tissue model, we found that NT-plasma treatment promoted both growth and differentiation of cartilaginous elements within the embryonic mouse autopod. Based on the lack of limb growth after NT-plasma treatment in an antioxidant environment, and the increase in H_2O_2-positive cells in and under the epithelia throughout the 6 day culture period, we propose that NT-plasma induction of intracellular ROS also plays a role in the growth and differentiation observed in the autopod. In addition, H_2O_2-positive cells were observed in the distal digit tips behind the AER, concurrent with enhanced Wnt signaling. These findings are consistent with the ROS dependence of signaling factors (e.g., Wnt, BMP, and FGF) required for autopod development.

The use of antioxidant treatment confirms that cellular production of ROS is required for normal growth and development of the limb autopod. However, very little has been reported on the direct contribution of ROS in autopod developmental examples of how ROS affects differentiation and development exists. *In vivo*, stem cells and adult MSCs have been reported to exist in a quiescent, glycolytic state with immature mitochondria.[35] Disruption of this environment by vascularization, growth factor binding, increased mitochondrial biogenesis, or external stresses induces elevations in ROS levels, leading to the induction of differentiation.[10] In addition, the requirement of ROS in the analogous process of regeneration was recently elucidated after tadpole tail amputation using fluorescent monitoring of H_2O_2.[36] In addition, regeneration in the nonmammalian systems, of both the axyotl salamander and *Xenopus* frog limbs, reports the most upregulated protein at 24 h after amputation is neuronal NOS.[37] A similar result to what we

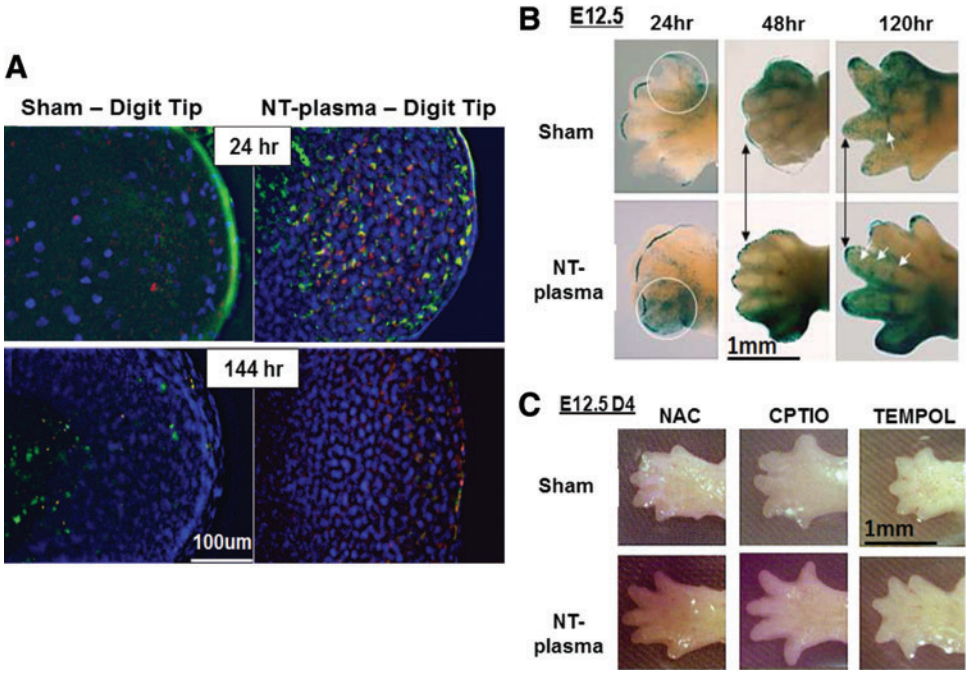

FIG. 5. NT-plasma treatment of E12.5 mouse autopods increases expression of chondrogenic and anti-oxidant genes and partially rescues antioxidant stunting. **(A)** H_2O_2-positive cells at the digit tip in sham (*left*) and NT-plasma (*right*)-treated limbs at 24 h (*top*) and 144 h (*bottom*). **(B)** Enhanced Wnt signaling is seen in the AER (*black arrows*) and presumptive joints (*white arrows*) of the NT-plasma-treated E12.5 autopod from the Wnt-signaling reporter mouse. **(C)** Pretreatment of E12.5 autopods with n-acetyl cysteine (NAC), 4-hydroxy-2,2,6,6-tetramethylpiperidin-1-oxyl (Tempol) or 2-(4-carboxyphenyl)-4,4,5,5-tetramethylimidazoline-1-oxyl-3-oxide (CPTIO) inhibitors stunts autopod morphogenesis. Treatment with NT-plasma partially rescues development, moderately enhancing digit morphogenesis compared with sham control. Color images available online at www.liebertpub.com/tea

observed at 24 h post-NT-plasma treatment was observed when eNOS expression was increased twofold above control in the mouse autopod. NO is known to trigger enhanced induction of vascular endothelial growth factor expression in cultured keratinocytes (HaCaT) and during cutaneous wound repair.[38,39] As stated earlier, increases in angiogenesis are known to enhance differentiation and undoubtedly play a role in enhancing autopod growth and development.

However, the fact that NT-plasma treatment showed some growth effect even in the presence of antioxidants indicates that ROS production may not be the sole mechanism driving enhanced autopod growth. A second possible reason that NT-plasma enhanced autopod growth was its inhibition of epithelial overgrowth. Epithelial overgrowth is commonly observed in organ culture systems, where direct contact with the nutrient-rich media favors cells on the outer layers of the tissue.[40,41] In limb regeneration, a thickening of the epidermis has been shown to inhibit signaling to the blastema, halting the regeneration process.[42–44] The observed decrease in epithelial thickening and increased limb growth after NT-plasma treatment supports this mechanism. One explanation for our findings is the presence and distribution of H_2O_2-positive cells throughout the culture period which indicates that the NT-plasma treatment has altered signaling and development within the epithelium.

Our study does not rule out the importance of other electrically induced changes, including changes in membrane permeability, bioelectric signaling, voltage-sensitive domains of transporter molecules, and/or the movement of calcium and other ions. Thus, it is possible that a combination of effects is at play in NT-plasma treatment. In addition to ROS and RNS, NT-plasma also generates charged ions, ozone, a pulsed electric field, and some UV and transmitted light. Pulsed electric fields have been reported to increase cell permeability, activate voltage-sensitive membrane channels, and mobilize calcium.[45,46] Mechanical and sonic forces are also generated by DBD plasmas.[21] Each of these modalities, applied in one way or another, have been reported to enhance differentiation of skeletal tissues[47] and cannot be ruled out as causative factors. Further study is needed to determine any role these other effects play in limb bud development.

Results of this study showing NT-plasma effects on limb autopod development suggest that this technology could be used to enhance tissue regeneration. This report, coupled with our previous work, solidifies the use of NT-plasma as a means to affect cellular differentiation and enhance tissue regeneration. Similar to other physical technologies currently in clinical use, EM fields and ultrasound, development of NT-plasma technology could provide enhanced outcomes for tissue engineering applications and regenerative medicine. How high-energy electrons produced by a NT-plasma discharge generate short-lived ROS and RNS to directly activate redox-sensitive signaling pathways thereby influencing cell signaling and precursor cell differentiation is only partially understood. Further exploration into biophysical interactions of NT-plasma with cells and tissues also enhances our understanding of cell behaviors to

promote the development of novel treatment modalities applied across many fields of study. NT-plasma is a new modality in biology and medicine, and its potential impact is yet to be determined.

Acknowledgments

Special thanks are due to Drs. Irving Shapiro, Maurizio Pacifici, Motomi Enomoto-Iwamoto, and Masahiro Iwamoto for their valuable discussions during the study. Special thanks are also due to Carol Diallo for laboratory support and Alex Fridman from the Drexel Plasma Institute for helpful insights on plasma conditions. This work was supported by NIH Grants 1 R01 EB 013011-01 (Freeman) and 5 R03 DE020840-03 (Freeman).

Disclosure Statement

No competing financial interests exist.

References

1. Steinbeck, M.J., Chernets, N., Zhang, J., Kurpad, D.S., Fridman, G., Fridman, A., *et al.* Skeletal cell differentiation is enhanced by atmospheric dielectric barrier discharge plasma treatment. PLoS One **8,** e82143, 2013.
2. Enomoto-Iwamoto, M., Kitagaki, J., Koyama, E., Tamamura, Y., Wu, C., Kanatani, N., *et al.* The Wnt antagonist Frzb-1 regulates chondrocyte maturation and long bone development during limb skeletogenesis. Dev Biol **251,** 142, 2002.
3. Koyama, E., Shibukawa, Y., Nagayama, M., Sugito, H., Young, B., Yuasa, T., *et al.* A distinct cohort of progenitor cells participates in synovial joint and articular cartilage formation during mouse limb skeletogenesis. Dev Biol **316,** 62, 2008.
4. Benazet, J.D., and Zeller, R. Dual requirement of ectodermal Smad4 during AER formation and termination of feedback signaling in mouse limb buds. Genesis **51,** 660, 2013.
5. Vasiliauskas, D., Laufer, E., and Stern, C.D. A role for hairy1 in regulating chick limb bud growth. Dev Biol **262,** 94, 2003.
6. Lee, Y., Grill, S., Sanchez, A., Murphy-Ryan, M., and Poss, K.D. Fgf signaling instructs position-dependent growth rate during zebrafish fin regeneration. Development **132,** 5173, 2005.
7. Oktyabrsky, O.N., and Smirnova, G.V. Redox regulation of cellular functions. Biochemistry (Mosc) **72,** 132, 2007.
8. Chamorro, M.N., Schwartz, D.R., Vonica, A., Brivanlou, A.H., Cho, K.R., and Varmus, H.E. FGF-20 and DKK1 are transcriptional targets of beta-catenin and FGF-20 is implicated in cancer and development. EMBO J **24,** 73, 2005.
9. Funato, Y., Michiue, T., Asashima, M., and Miki, H. The thioredoxin-related redox-regulating protein nucleoredoxin inhibits Wnt-beta-catenin signalling through dishevelled. Nat Cell Biol **8,** 501, 2006.
10. Chen, C., Liu, Y., Liu, R., Ikenoue, T., Guan, K.L., and Zheng, P. TSC-mTOR maintains quiescence and function of hematopoietic stem cells by repressing mitochondrial biogenesis and reactive oxygen species. J Exp Med **205,** 2397, 2008.
11. Chen, C.-T., Hsu, S.-H., and Wei, Y.-H. Upregulation of mitochondrial function and antioxidant defense in the differentiation of stem cells. Biochim Biophys Acta **1800,** 257, 2010.
12. Chen, C.-T., Shih, Y.-R.V., Kuo, T.K., Lee, O.K., and Wei, Y.-H. Coordinated changes of mitochondrial biogenesis and antioxidant enzymes during osteogenic differentiation of human mesenchymal stem cells. Stem Cells **26,** 960, 2008.
13. Ji, A.-R., Ku, S.-Y., Cho, M.S., Kim, Y.Y., Kim, Y.J., Oh, S.K., *et al.* Reactive oxygen species enhance differentiation of human embryonic stem cells into mesendodermal lineage. Exp Mol Med **42,** 175, 2010.
14. Yanes, O., Clark, J., Wong, D.M., Patti, G.J., Sanchez-Ruiz, A., Benton, H.P., *et al.* Metabolic oxidation regulates embryonic stem cell differentiation. Nat Chem Biol **6,** 411, 2010.
15. Schnabel, D., Salas-Vidal, E., Narvaez, V., Sanchez-Carbente Mdel, R., Hernandez-Garcia, D., Cuervo, R., *et al.* Expression and regulation of antioxidant enzymes in the developing limb support a function of ROS in interdigital cell death. Dev Biol **291,** 291, 2006.
16. Salas-Vidal, E., Lomeli, H., Castro-Obregon, S., Cuervo, R., Escalante-Alcalde, D., and Covarrubias, L. Reactive oxygen species participate in the control of mouse embryonic cell death. Exp Cell Res **238,** 136, 1998.
17. Rong, Y., Doctrow, S.R., Tocco, G., and Baudry, M. EUK-134, a synthetic superoxide dismutase and catalase mimetic, prevents oxidative stress and attenuates kainate-induced neuropathology. Proc Natl Acad Sci U S A **96,** 9897, 1999.
18. Jung, C., Rong, Y., Doctrow, S., Baudry, M., Malfroy, B., and Xu, Z. Synthetic superoxide dismutase/catalase mimetics reduce oxidative stress and prolong survival in a mouse amyotrophic lateral sclerosis model. Neurosci Lett **304,** 157, 2001.
19. Siemens, C.W. On the electrical tests employed during the construction of the malta and alexandria telegraph, and on insulating and protecting submarine cables. J Franklin Inst **74,** 166, 1862.
20. Eliasson, B., Egli, W., and Kogelschatz, U. Modelling of dielectric barrier discharge chemistry. Pure Appl Chem **66,** 1275, 1994.
21. Fridman, A., and Friedman, G. Plasma Medicine. 2 ed. West Sussex, UK: Wiley & Sons, Incorporated, 2013.
22. Parivar, K., Kouchesfehani, M.H., Boojar, M.M., and Hayati, R.N. Organ culture studies on the development of mouse embryo limb buds under EMF influence. Int J Radiat Biol **82,** 455, 2006.
23. Freeman, T.A., Patel, P., Parvizi, J., Antoci, V., Jr., and Shapiro, I.M. Micro-CT analysis with multiple thresholds allows detection of bone formation and resorption during ultrasound-treated fracture healing. J Orthop Res **27,** 673, 2009.
24. Griffin, M., and Bayat, A. Electrical stimulation in bone healing: critical analysis by evaluating levels of evidence. Eplasty **11,** e34, 2011.
25. DasGupta, R., and Fuchs, E. Multiple roles for activated LEF/TCF transcription complexes during hair follicle development and differentiation. Development **126,** 4557, 1999.
26. Lobe, C.G., Koop, K.E., Kreppner, W., Lomeli, H., Gertsenstein, M., and Nagy, A. Z/AP, a double reporter for cre-mediated recombination. Dev Biol **208,** 281, 1999.
27. Iwamoto, M., Tamamura, Y., Koyama, E., Komori, T., Takeshita, N., Williams, J.A., *et al.* Transcription factor ERG

and joint and articular cartilage formation during mouse limb and spine skeletogenesis. Dev Biol **305,** 40, 2007.
28. Ueta, C., Iwamoto, M., Kanatani, N., Yoshida, C., Liu, Y., Enomoto-Iwamoto, M., *et al.* Skeletal malformations caused by overexpression of Cbfa1 or its dominant negative form in chondrocytes. J Cell Biol **153,** 87, 2001.
29. Fridman, G., Peddinghaus, M., Ayan, H., Fridman, A., Balasubramanian, M., Gutsol, A., *et al.* Blood coagulation and living tissue sterilization by floating-electrode dielectric barrier discharge in air. Plasma Chem Plasma Proc **26,** 425, 2006.
30. Parr, B.A., and McMahon, A.P. Dorsalizing signal Wnt-7a required for normal polarity of D-V and A-P axes of mouse limb. Nature **374,** 350, 1995.
31. Parasassi, T., Brunelli, R., Costa, G., De Spirito, M., Krasnowska, E.K., Lundeberg, T., *et al.* Thiol redox transitions in cell signaling: a lesson from N-acetylcysteine. Sci World J **10,** 1192, 2010.
32. Castagna, R., Davis, P.A., Vasu, V.T., Soucek, K., Cross, C.E., Greci, L., *et al.* Nitroxide radical TEMPO reduces ozone-induced chemokine IL-8 production in lung epithelial cells. Toxicol In Vitro **23,** 365, 2009.
33. Suy, S., Mitchell, J.B., Ehleiter, D., Haimovitz-Friedman, A., and Kasid, U. Nitroxides tempol and tempo induce divergent signal transduction pathways in MDA-MB 231 breast cancer cells. J Biol Chem **273,** 17871, 1998.
34. Pieper, G.M., and Siebeneich, W. Use of a nitronyl nitroxide to discriminate the contribution of nitric oxide radical in endothelium-dependent relaxation of control and diabetic blood vessels. J Pharmacol Exp Ther **283,** 138, 1997.
35. Fischer, L.J., McIlhenny, S., Tulenko, T., Golesorkhi, N., Zhang, P., Larson, R., *et al.* Endothelial differentiation of adipose-derived stem cells: effects of endothelial cell growth supplement and shear force. J Surg Res **152,** 157, 2009.
36. Love, N.R., Chen, Y., Ishibashi, S., Kritsiligkou, P., Lea, R., Koh, Y., *et al.* Amputation-induced reactive oxygen species are required for successful *Xenopus* tadpole tail regeneration. Nat Cell Biol **15,** 222, 2013.
37. Grow, M., Neff, A.W., Mescher, A.L., and King, M.W. Global analysis of gene expression in *Xenopus* hindlimbs during stage-dependent complete and incomplete regeneration. Dev Dyn **235,** 2667, 2006.
38. Frank, S., Stallmeyer, B., Kampfer, H., Kolb, N., and Pfeilschifter, J. Nitric oxide triggers enhanced induction of vascular endothelial growth factor expression in cultured keratinocytes (HaCaT) and during cutaneous wound repair. FASEB J **13,** 2002, 1999.
39. Stallmeyer, B., Kampfer, H., Kolb, N., Pfeilschifter, J., and Frank, S. The function of nitric oxide in wound repair: inhibition of inducible nitric oxide-synthase severely impairs wound reepithelialization. J Invest Dermatol **113,** 1090, 1999.
40. Browning, T.H., and Trier, J.S. Organ culture of mucosal biopsies of human small intestine. J Clin Invest **48,** 1423, 1969.
41. Hoffman, D.S., Bringas, P., Jr., and Slavkin, H.C. Coculture of contiguous developmental fields in a serumless, chemically-defined medium: an *in vitro* model permissive for coordinate development of the mouse ear. Int J Dev Biol **40,** 953, 1996.
42. Mescher, A.L. Effects on adult newt limb regeneration of partial and complete skin flaps over the amputation surface. J Exp Zool **195,** 117, 1976.
43. Neufeld, D.A., and Day, F.A. Perspective: a suggested role for basement membrane structures during newt limb regeneration. Anat Rec **246,** 155, 1996.
44. Neufeld, D.A., Day, F.A., and Settles, H.E. Stabilizing role of the basement membrane and dermal fibers during newt limb regeneration. Anat Rec **245,** 122, 1996.
45. Scarlett, S.S., White, J.A., Blackmore, P.F., Schoenbach, K.H., and Kolb, J.F. Regulation of intracellular calcium concentration by nanosecond pulsed electric fields. Biochim Biophys Acta **1788,** 1168, 2009.
46. Pall, M.L. Electromagnetic fields act via activation of voltage-gated calcium channels to produce beneficial or adverse effects. J Cell Mol Med **17,** 958, 2013.
47. Goodman, R., Lin-Ye, A., Geddis, M.S., Wickramaratne, P.J., Hodge, S.E., Pantazatos, S.P., *et al.* Extremely low frequency electromagnetic fields activate the ERK cascade, increase hsp70 protein levels and promote regeneration in Planaria. Int J Radiat Biol **85,** 851, 2009.

Address correspondence to:
Theresa A. Freeman, PhD
Department of Orthopaedic Surgery
Thomas Jefferson University
501 Curtis Bldg., 1015 Walnut Street
Philadelphia, PA 19107

E-mail: theresa.freeman@jefferson.edu

Received: January 15, 2014
Accepted: July 23, 2014
Online Publication Date: September 16, 2014